Genes, Brain and Behavior
Official publication of the International Behavioural and Neural Genetics Society

Genes, Brain and Behavior (2014) ***13:*** *675–685* doi: 10.1111/gbb.12157

A genome-wide search for quantitative trait loci affecting the cortical surface area and thickness of Heschl's gyrus

D.-C. Cai[*,†,‡,§,¶], H. Fonteijn[‡,§], T. Guadalupe[‡], M. Zwiers[§,], K. Wittfeld[††], A. Teumer[‡‡], M. Hoogman[‡,§,**], A. Arias-Vásquez[§,**], Y. Yang[†], J. Buitelaar[§,**], G. Fernández[§,**], H. G. Brunner[§,**], H. van Bokhoven[§,**], B. Franke[§,**], K. Hegenscheid[§§], G. Homuth[¶¶], S. E. Fisher[‡,§], H. J. Grabe[††,***], C. Francks[‡,§] and P. Hagoort[*,‡,§]**

[†] Institute of Psychology, Chinese Academy of Sciences, Beijing, China, [‡] Max Planck Institute for Psycholinguistics, [§] Donders Institute for Brain, Cognition and Behaviour, Radboud University Nijmegen, Nijmegen, The Netherlands, [¶] Graduate University of Chinese Academy of Sciences, Beijing, China, [**] Departments of Human Genetics, Psychiatry and Cognitive Neuroscience, Radboud University Nijmegen Medical Centre, Nijmegen, The Netherlands, [††] German Center for Neurodegenerative Diseases (DZNE), Rostock/Greifswald, Greifswald, Germany, [‡‡] Institute for Community Medicine, [§§] Institute for Radiology, [¶¶] Interfaculty Institute for Genetics and Functional Genomics, University Medicine Greifswald, Greifswald, and [***] Department of Psychiatry and Psychotherapy, University Medicine Greifswald, HELIOS Hospital Stralsund, Stralsund, Germany

**Corresponding authors: D.-C. Cai, Institute of Psychology, 16 Lincui Road, Chaoyang District, Beijing 100101, China. E-mail: danchao.cai@outlook.com and P. Hagoort, Max Planck Institute for Psycholinguistics, Wundtlaan 1, Nijmegen 6525 XD, The Netherlands. E-mail: peter.hagoort@mpi.nl*

Heschl's gyrus (HG) is a core region of the auditory cortex whose morphology is highly variable across individuals. This variability has been linked to sound perception ability in both speech and music domains. Previous studies show that variations in morphological features of HG, such as cortical surface area and thickness, are heritable. To identify genetic variants that affect HG morphology, we conducted a genome-wide association scan (GWAS) meta-analysis in 3054 healthy individuals using HG surface area and thickness as quantitative traits. None of the single nucleotide polymorphisms (SNPs) showed association *P* values that would survive correction for multiple testing over the genome. The most significant association was found between right HG area and SNP rs72932726 close to gene *DCBLD2* (3q12.1; $P = 2.77 \times 10^{-7}$). This SNP was also associated with other regions involved in speech processing. The SNP rs333332 within gene *KALRN* (3q21.2; $P = 2.27 \times 10^{-6}$) and rs143000161 near gene *COBLL1* (2q24.3; $P = 2.40 \times 10^{-6}$) were associated with the area and thickness of left HG, respectively. Both genes are involved in the development of the nervous system. The SNP rs7062395 close to the X-linked deafness gene *POU3F4* was associated with right HG thickness (Xq21.1; $P = 2.38 \times 10^{-6}$). This is the first molecular genetic analysis of variability in HG morphology.

Keywords: Auditory network, genetics, genome-wide association scan, Heschl's gyrus, language network, magnetic resonance imaging, speech processing, surface-based

Received 7 April 2014, revised 10 July 2014, accepted for publication 24 July 2014

Heschl's gyrus (HG) is a macro-anatomical landmark of the brain which contains the primary auditory cortex and is cytoarchitectonically identified as Brodmann Area 41 (Morosan *et al.* 2001). It is located at the posterior end of the superior temporal gyrus (STG) and distinguishes itself from other gyri by running in the posteromedial–anterolateral direction. The size of HG varies substantially between individuals (Abdul-Kareem & Sluming 2008). In addition, the left HG is on average 10–30% larger than the right HG (Smiley *et al.* 2013). This asymmetry is related to left hemisphere dominance in speech and language processing (Penhune *et al.* 1996).

Previous studies have indicated a central role of HG in pitch perception (Krumbholz *et al.* 2003) and sound-level perception (Hart *et al.* 2002). Increased white matter (WM) and gray matter (GM) volumes in HG, especially the left HG, have been reported in individuals who show high ability in speech perception, such as fast learners of foreign speech contrasts (Golestani & Pallier 2007) and linguistic tones (Wong *et al.* 2008), bilinguals (Ressel *et al.* 2012) and phoneticians (Golestani *et al.* 2011). Similarly, a larger GM volume in HG, particularly the right HG, has been found in musicians compared with non-musicians (Schneider *et al.* 2002). People with more musical experience tend to have a larger GM volume of the left HG (Gaser & Schlaug 2003). Furthermore, professional musicians with absolute pitch have a larger right HG than musicians who do not (Wengenroth *et al.* 2013). Functional imaging studies also support the role of HG as a pitch processing center. Pure tones with higher pitch mainly activate the anterior and posterior part of HG, while the activation for lower tones is more centered around the middle part of HG (Da Costa *et al.* 2011). Sounds with pitch information evoke stronger brain activation than those without pitch in the lateral part of HG and the neighboring planum temporale (Patterson *et al.* 2002; Puschmann *et al.* 2010).

A positive correlation between HG size and proficiency of auditory processing is of great interest as it links brain structure to behavioral performance. However, it does not indicate whether differences in brain structure and behavioral performance are linked because of pleiotropic genetic variation, as opposed to being driven by experience or training. Golestani *et al.* (2011) demonstrated that there was no correlation between the GM volume in HG and the length of time spent in professional training by phoneticians. This suggests that the HG volume differences observed between phoneticians and non-phoneticians arise before training and that those differences might be partly explained by genetic variations. Moreover, imaging studies in twins have shown that the morphology of HG is highly heritable (Peper *et al.* 2007). The heritabilities of HG area and thickness derived from surface-based representations were reported to be 0.73 and 0.71, respectively (Winkler *et al.* 2010). Another twin study showed that the heritabilities of HG area and thickness were 0.30 and 0.50, respectively, when using vertex-based estimates (Eyler *et al.* 2012).

Given its correlation with behavioral performance on sound perception and its relatively high heritability, it is important to better understand the genetic underpinnings of the morphology of HG. To this end, we conducted genome-wide association scan (GWAS) meta-analysis in order to identify genetic variants that affect HG morphology, as assessed from magnetic resonance imaging (MRI) data in 3054 participants. In a GWAS analysis, millions of single nucleotide polymorphisms (SNPs) covering the whole genome are tested individually for their association with a trait. The large number of statistical tests in GWAS necessitates stringent thresholds to avoid type I errors. In addition, the genetic effects are expected to explain only a limited proportion of the overall trait variability. As a result, large sample sizes are required to detect significant effects in GWAS studies. Fully automated algorithms are therefore necessary for the segmentation and parcellation of HG. Of the different automated measures available, cortical volume is commonly used in functional MRI studies concerning HG (Abdul-Kareem & Sluming 2008). However, it has been shown that measures of regional cortical volume conflate variability in surface area and thickness, which are partially genetically independent from each other (Panizzon *et al.* 2009; Winkler *et al.* 2010). We therefore analyzed surface area and thickness as separate phenotypes. Considering the asymmetry of HG (Smiley *et al.* 2013), we allowed for the effect sizes of SNPs to be different in both hemispheres. As a result, we conducted four separate GWAS on the surface area and thickness of both left and right HG. We used the results to identify novel candidate loci associated with HG morphology.

Material and methods

Participants

We included 3054 participants (56.0% females) from two independent imaging genetics studies. The Brain Imaging Genetics (BIG) project is based at Nijmegen, The Netherlands (Franke *et al.* 2010). At the time of this study, it included 2483 healthy individuals aged 18–35 years (53.2% females, mean age = 26.8 ± 12.0 years). Genome-wide genotype data were available for 1276 participants (57.4% females, mean age = 23.0 ± 3.8 years). All of the participants were part of other brain imaging studies conducted at the Donders Centre for Cognitive Neuroimaging, Nijmegen. Informed consent for the participation in the BIG project was given separately from the original imaging studies. Saliva samples were then collected for DNA analysis. The study was approved by the local medical ethics committee (CMO regio Arnhem/Nijmegen).

The Study of Health in Pomerania (SHIP) is a population-based project conducted in Greifswald, Germany (Volzke *et al.* 2011). SHIP-0 consisted of adult German residents in northeastern Germany. A two-stage stratified cluster sample (aged 20–79 years at baseline) was randomly drawn from local registries. A total of 4308 Caucasians participated at baseline SHIP-0 (1997–2001). The first follow-up examination (SHIP-1, $N = 3300$) was conducted 5 years later. The second follow-up examination (SHIP-2, $N = 2333$) was carried out about 10 years after baseline. Concurrent with SHIP-2, a new independent sample (SHIP-Trend-0, $N = 4420$) in the same area was drawn in 2008 and similar examinations were undertaken. Participants in both cohorts underwent a whole-body MRI scan, as well as genotyping for common polymorphisms. In this study, we used the data from SHIP-2 and SHIP-TREND-0 (hereafter referred as SHIP-T). Participants with neurological deficits such as stroke, tumors, epilepsy and hydrocephalus were further excluded. As a result, 1014 participants from SHIP-2 (59.2% females, mean age = 55.2 ± 12.6 years) and 1937 participants from SHIP-T (52.6% females, mean age = 50.6 ± 13.9 years) remained for further analysis. Genotypes were available for 956 participants in SHIP-2 (53.6% females) and 822 participants in SHIP-T (56.6% females).

Data acquisition and processing

Structural imaging data in the BIG project were obtained with three scanners: a 1.5-T Siemens Sonata scanner ($N = 444$), a 1.5-T Siemens Avanto scanner ($N = 931$) and a 3-T Siemens Trio scanner ($N = 1108$). For the GWAS sample, 49.6% of the participants were scanned using the 1.5-T scanners. The parameters used were slight variations of a standard T1-weighted 3D magnetization prepared rapid gradient echo (MPRAGE; voxel size = $1.0 \times 1.0 \times 1.0\,mm^3$) due to the different designs of the functional studies from which these data were taken. The most common combinations of repetition time (in milliseconds), echo time (in milliseconds) and flip angle (and their frequencies) were 2300/3.03/8° (30%), 2250/2.95/15° (26%), 2250/3.68/15° (13%) and 2730/2.95/7° (11%). Imaging data in the SHIP project were obtained in a 1.5-T Siemens Avanto scanner using the standard T1-weighted MPRAGE sequence with following parameters: repetition time = 1900 milliseconds, echo time = 3.4 milliseconds, flip angle = 15°, voxel size = $1.0 \times 1.0 \times 1.0\,mm^3$ (Hegenscheid *et al.* 2009).

Preprocessing and parcellation of T1 images were performed in FreeSurfer (v5.3 in BIG and v5.1 in SHIP) with the default 'recon-all' pipeline (Fischl *et al.* 2004). The preprocessing began with motion correction, intensity normalization and skull stripping. White matter voxels were then segmented based on their locations and intensities. A mesh was built around the resulting WM volume and smoothed. Topological defects were automatically corrected. The boundary between WM and GM was smoothed again to obtain the WM surface. The pial surface was produced by nudging the WM surface outwards until the point with the maximal tissue contrast was reached. Cortical thickness was then defined as the distance between the WM and pial surface. After the surface model was constructed, the surfaces were parcellated into regions using an atlas-based procedure (Desikan *et al.* 2006). From this parcellation, we then extracted the mean cortical surface area and thickness of bilateral HG. We controlled for potential effects of age, sex, handedness, total brain volume and field strength using linear regression in *R* (v2.15.2 in BIG and v2.12.2 in SHIP, http://www.R-project.org). We adjusted for the total brain volume to increase sensitivity to detect effects that are particularly relevant for HG. Field strength was adjusted because it had an effect on FreeSurfer-measured traits in the BIG dataset (see the ENIGMA protocol; Stein *et al.* 2012).

Repeatability analysis

To assess the reliability of FreeSurfer measures in this analysis, we analyzed the scan–rescan correlations of HG surface area and thickness, using data from 290 twice-scanned participants in the BIG dataset. The Pearson correlations between the first and second scans were calculated in *R* v2.15.2.

GWAS analysis

The BIG and SHIP-2 samples were genotyped with the Affymetrix Genome-Wide Human SNP Array 6.0, while the SHIP-T samples were genotyped with the Illumina Human Omni 2.5 array. The exclusion threshold for the genotyping call rate was 90%, 92% and 94% for BIG, SHIP-2 and SHIP-T, respectively. Imputation against the 1000 Genomes (v3) reference panel was performed with the software MINIMAC and IMPUTE (v2.2.2), respectively, for the BIG and SHIP samples. More details for genotyping can be found elsewhere for BIG (Guadalupe *et al.* 2014) and SHIP (Teumer *et al.* 2013). Genome-wide association scan analyses on the surface area and thickness of bilateral HG were carried out separately in each dataset using the linear regression option in PLINK v1.07 (Purcell *et al.* 2007). SNPs with a minor allele frequency (MAF) ≤ 0.05, with a genotype call rate $\leq 95\%$, or that were out of Hardy–Weinberg equilibrium ($P \leq 5 \times 10^{-6}$) were excluded from the analyses.

To merge the genetic association results across three datasets, we conducted sample-size-based meta-analyses in METAL (Willer *et al.* 2010). For each SNP, this analysis combines the probabilities of a genetic effect (i.e. *P* values from linear regression) from each dataset based on the sample size and the direction of effect. Only SNPs present in all three datasets were included. In the final meta-analyses, we analyzed 4 103 035 SNPs in 3054 individuals. The genome-wide significance threshold was set to 5×10^{-8} according to the community standard (Barsh *et al.* 2012). For a meta-analysis of this sample size, there was ≥80% power to detect variants with effect size of 1.32% of the variance for MAF ≥ 0.05 at $P < 5 \times 10^{-8}$ (Purcell *et al.* 2003).

Candidate gene analysis

The GWAS analysis provided the opportunity to assess specific candidate variants and genes indicated by earlier genetic studies which examined traits relevant to the current phenotypes. We searched for genetic studies of pitch or tone perception, cortical surface area and thickness, and found the following studies that reported significant results (till March 2014).

A genome-wide linkage and association analysis was conducted on music aptitude in 76 extended Finnish families, including the ability to discriminate pitch, duration and sound pattern (Oikkonen *et al.* 2014). The most significant association was found between rs9854612 (near gene *GATA2* at 3q21.3) and the combined score of the three abilities. The highest probability of linkage was obtained for pitch perception ability near gene *PCDH7*, and the strongest associations in this region were found for SNPs rs13146789 and rs13109270 (4p14). Another genome-wide linkage study of 212 healthy siblings used magnetoencephalographic responses to pure tones as phenotypes (Renvall *et al.* 2012). Significant linkage was found at 2q37 together with suggestive linkages at 3p12 and 8q24. Within the linkage region of 3p12, gene *ROBO1* plays a role in interaural interaction in auditory pathways (Lamminmaki *et al.* 2012). Two other candidates came from studies investigating the use of tone languages, as it has been shown that experience with linguistic tones can influence non-linguistic pitch perception (Gandour *et al.* 1998; Peng *et al.* 2013). The allele frequencies of SNP rs41310927 in gene *ASPM* and rs930557 in gene *MCPH1* were suggested to be associated with the use of tone languages when compared across world populations (Dediu & Ladd 2007). The *ASPM* SNP was further associated with behavioral performance and functional brain activation in linguistic tone perception (Wong *et al.* 2012), although the sample size in this study was very small (13 participants for imaging genetics), and the effect was in the opposite direction to that reported by Dediu and Ladd (2007).

There are few genetic association studies that have used cortical surface area or thickness as traits. The SNP rs2239464 within gene *MECP2* was significantly associated with the cortical surface area throughout the cortex (Joyner *et al.* 2009). The SNP rs4906844 and rs11633924, within a putative protein-coding gene *LOC100128714* at 15q12, showed significant association with average cortical thickness (over all cortical regions) and modest association with cognitive performance including verbal learning and verbal fluency (Bakken *et al.* 2011). Cortical thickness was also studied in a whole-genome quantitative trait locus analysis that integrated data on gene expression (Kochunov *et al.* 2011). The expression levels of genes *RORA, ADM10* and *NARG2* were significantly correlated with GM thickness.

For the genes mentioned above, we calculated the gene-level *P* values in KGG v2.5 (Li *et al.* 2010). The SNP level statistics were combined using the extended Simes test (known as GATES, Li *et al.* 2011). The association between the individual SNPs mentioned and HG phenotypes were also examined. Proxy SNPs in high linkage disequilibrium ($r^2 > 0.8$) were used when the candidate SNPs were not available in the GWAS results.

Hearing loss is a common sensory disorder that can be associated with changes in the structure of HG and the auditory cortex. Morphometric analysis showed that congenitally deaf subjects had a greater GM–WM ratio bilaterally in HG (Emmorey *et al.* 2003). As a complex trait, deafness has many different subtypes relating to different genetic variants. In this analysis, we included 46 genes implicated in non-syndromic deafness as summarized in Hilgert *et al.* (2009). Gene-level *P* values were calculated for each of these genes. Seven of them were not included in the NCBI36/hg18 genome assembly that was used in KGG for the calculation of gene-level *P* values.

We also considered schizophrenia as a potential trait linked to HG variation. Bilateral volume reductions were reported in schizophrenia patients (Smiley 2009). The severity of auditory hallucinations and delusions in people with schizophrenia was correlated with volume loss in the left HG (Gaser *et al.* 2004). We assessed 24 genome-wide significant SNPs reported in a recent large-scale meta-analysis (Ripke *et al.* 2013). To combine the effect size of these SNPs, we also calculated a putative schizophrenia genetic risk score by adding up the number of reference alleles in each SNP which were weighted by the logarithm of the odds ratio (Purcell *et al.* 2009). The correlation between the risk score and the current phenotypes was examined in the BIG dataset.

Explorative analysis across the cerebral cortex

To further investigate whether the most significant genetic variant arising from GWAS (an effect on HG surface area, see below) was affecting HG specifically or also associated with morphological variations in other regions of the cerebral cortex, we tested the effects of this SNP on the surface areas of all 68 regions within the Desikan atlas, in the same three datasets as used for GWAS.

Results

The mean surface areas of left and right HG were 464.67 and 349.64 mm^2, respectively (Table 1). The correlation between left and right HG area was 0.42, 0.38 and 0.39 for BIG, SHIP-2 and SHIP-T, respectively. The mean cortical thickness of left and right HG were 2.342 and 2.363 mm, respectively. The correlation between left and right HG thickness was 0.65, 0.59 and 0.60 for BIG, SHIP-2 and SHIP-T, respectively.

Repeatability analysis

The scan–rescan correlation of HG surface area was 0.8954 in the left and 0.8983 in the right hemisphere. As for the average thickness, the scan–rescan correlations were 0.7662 and 0.7468 for left and right HG, respectively.

GWAS analysis

No SNP showed genome-wide significant association with the area of either left or right HG (Fig. 1). Suggestive loci

Table 1: Descriptive statistics on the HG measures

	BIG	SHIP-2	SHIP-T
Number of individuals	2483	1014	1937
Mean age ± SD (years)	26.8 ± 12.0	55.2 ± 12.6	50.6 ± 14.0
Mean area ± SD (mm^2)			
Left HG	472.38 ± 81.56	457.47 ± 79.67	458.56 ± 76.38
Right HG	356.35 ± 63.16	342.72 ± 59.21	344.68 ± 57.47
Mean thickness ± SD (mm)			
Left HG	2.445 ± 0.255	2.232 ± 0.234	2.267 ± 0.229
Right HG	2.465 ± 0.255	2.250 ± 0.250	2.292 ± 0.246

with $P < 1 \times 10^{-5}$ are listed in Table 2. The most significant association with the area of left HG was found at rs333332 within gene *KALRN* (3q21.2; $P = 2.27 \times 10^{-6}$; MAF = 0.33). The standardized regression coefficients were −0.17, −0.10 and −0.04 for BIG, SHIP-2 and SHIP-T, explaining 1.29%, 0.45% and 0.06% of the variance, respectively. The association between rs333332 and right HG area was not significant ($P = 0.0962$). The top SNP found in right HG area was rs72932726 near gene *DCBLD2* (3q12.1; $P = 2.77 \times 10^{-7}$; MAF = 0.11). The standardized regression coefficients were 0.22, 0.14 and 0.16 for BIG, SHIP-2 and SHIP-T, explaining 0.86%, 0.46% and 0.50% of the variance, respectively. rs72932726 was also associated to a lesser extent with left HG area ($P = 7.84 \times 10^{-4}$).

No genome-wide significant association was found in the analyses of cortical thickness (Fig. 1). Suggestive loci with $P < 1 \times 10^{-5}$ are listed in Table 3. The SNP rs143000161 near gene *COBLL1* showed the most significant association with the thickness of left HG (2q24.3; $P = 2.40 \times 10^{-6}$; MAF = 0.08). The standardized regression coefficients were 0.06, 0.04 and 0.05 for BIG, SHIP-2 and SHIP-T, explaining 0.73%, 0.49% and 0.67% of the variance, respectively. rs143000161 was associated with right HG thickness to a lesser extent ($P = 0.0013$). The most significant SNP associated with the thickness of right HG was rs7062395 near the gene *POU3F4* (Xq21.1; $P = 2.38 \times 10^{-6}$; MAF = 0.19). The standardized regression coefficients were −0.03, −0.05 and −0.05 for BIG, SHIP-2 and SHIP-T, explaining 0.50%, 1.08% and 1.13% of the variance, respectively. There was a weak association of rs7062395 with left HG thickness ($P = 0.0233$).

Candidate gene analysis

We included nine SNPs and eight genes from pitch/tone studies and cortical surface/thickness studies. None of them showed significant association with the HG measures after correction for multiple comparisons (Table S2, Supporting Information). One SNP (rs9854612 near gene *GATA2*) was nominally significant ($P = 0.041$), which was previously associated with the combined ability in discriminating pitch, duration and sound pattern.

For the available hearing loss candidate genes, none of the gene-level *P* values were significant after correction for multiple comparisons (Table S3).

For the candidate SNPs related to schizophrenia, one of them (rs7085104) was marginally significant after correction for all the 33 candidate SNPs tested (Table S4). The uncorrected *P* values for left area, right area, left thickness and right thickness were 0.0017, 0.0171, 0.0042 and 0.0262, respectively. No significant correlation was found between the schizophrenia genetic risk score and the HG measures (Fig. S3).

Brain-wide explorative analysis

The most significant association from GWAS was found between rs72932726 and right HG area (3q12.1; $P = 2.77 \times 10^{-7}$; MAF = 0.11). We tested this SNP against the surface area of all other cortical regions defined in the Desikan atlas. In addition to the right HG, rs72932726 showed significant association with the surface area of bilateral superior frontal gyrus (SFG), bilateral STG, left middle temporal gyrus (MTG), right pars orbitalis and left HG (although not significant in the GWAS), after Bonferroni correction for all regions in the Desikan atlas (Table 4).

Discussion

In this study, we conducted GWAS analyses on the cortical surface area and cortical thickness of left and right HG. None of the SNPs showed genome-wide significant association with the HG measures. The most significant association we found was between the area of right HG and rs72932726. This SNP is near the protein-coding gene *DCBLD2* (discoidin, CUB and LCCL domain containing 2). *DCBLD2* encodes a type I transmembrane protein that is highly expressed in nerve bundles and vascular smooth muscle cells. It may be involved in a wide range of functions in the nervous and vascular systems (Kobuke *et al.* 2001; Sadeghi *et al.* 2007). *DCBLD2* has also been identified as part of a complex epidermal growth factor (EGF) phosphotyrosine signaling network, serving as a novel tyrosine phosphorylation target of EGF signaling in human cancer cells (Chen *et al.* 2007).

The same SNP was also associated with variations in surface areas of left HG, bilateral STG, left MTG, left SFG and right pars orbitalis (Fig. 2). These regions are part of two closely related functional networks: the auditory network and the language network, which is consistent with the idea that regions within functional networks might be subject to

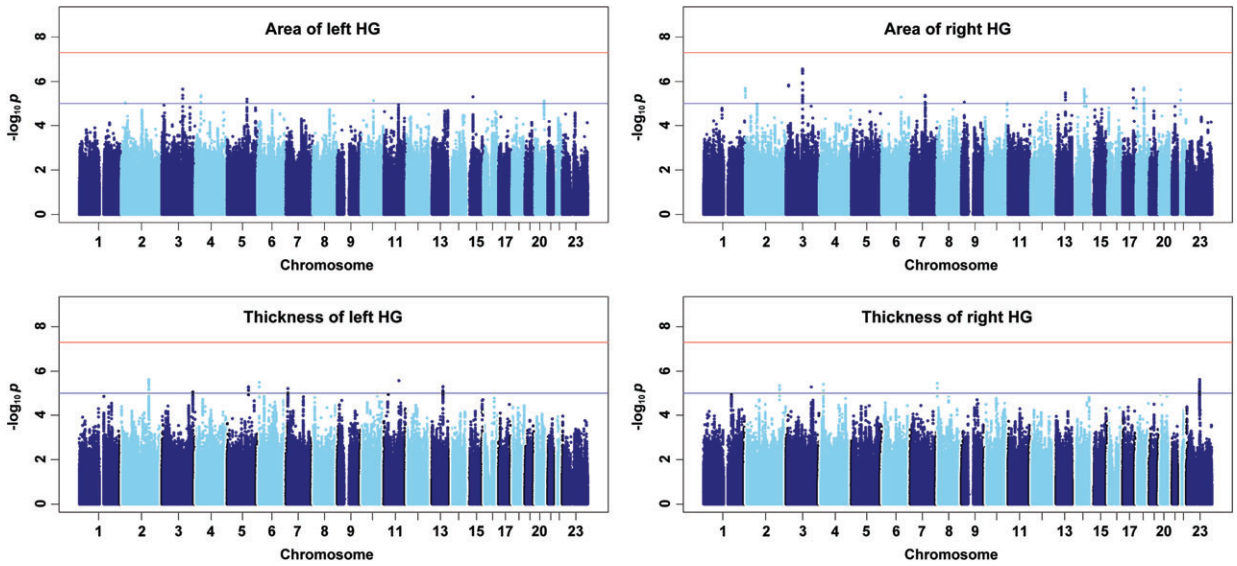

Figure 1: Manhattan plots for the association of 4 103 035 SNPs to the morphology of left and right HG in 3054 participants. The horizontal axis shows the base pair position of each SNP and the vertical axis shows the $-\log_{10}$ of the *P* value for association. The blue and red horizontal lines indicate suggestive ($P < 1 \times 10^{-5}$) and significant ($P < 5 \times 10^{-8}$) thresholds, respectively. See Figure S1 for Manhattan plots and Figure S2 for QQ plots for individual datasets.

shared genetic influences. Analyses of resting-state functional connectivity show that STG is strongly connected to HG, and that they form the main components of the auditory network (Kang *et al.* 2011). Moreover, an analysis of structural covariation (correlation of surface area across regions) in the current datasets showed that the ipsilateral STG was the region with the highest correlation with HG ($R = 0.45$ and 0.41 in left and right hemispheres, respectively, after correction for covariates), providing further evidence for their involvement in the same functional network. Heschl's gyrus and STG are bilaterally activated during both speech and non-speech sound processing (Hickok & Poeppel 2007; Price 2012) and are thought to be involved in the early processing of complex sounds. During speech processing, the output from bilateral HG and dorsal STG is further processed by regions in the language network. These later processing stages include word retrieval with minimal semantics in the posterior STG and the retrieval of higher level semantic information in left MTG. Subsequently, the dorsal part of left SFG is involved in selecting and retrieving semantic attributes based on context (Price 2012; Scott *et al.* 2003). The right pars orbitalis as part of the right inferior frontal gyrus is involved in unifying the world knowledge and local context during discourse comprehension (Menenti *et al.* 2009). In other words, rs72932726 is associated with structural variation in multiple brain regions that are involved in speech and language processing. This suggests that brain regions that form functional networks are also (at least partially) under common genetic control. It would therefore be interesting in future studies to further investigate the genetic underpinnings of the shared variance between brain regions, for instance by considering multivariate approaches (Ferreira & Purcell 2009).

The SNP that showed the most significant association with left HG area (rs333332) is located within the protein-coding gene *KALRN* (kalirin, RhoGEF kinase). Kalirin is highly expressed in the central nervous system (Rabiner *et al.* 2005). It plays an important role in regulating axonal growth and dendritic morphogenesis and is essential for neuronal maintenance, brain connectivity (May *et al.* 2002; Rabiner *et al.* 2005) and implicated in disorders such as schizophrenia (Glausier & Lewis 2013), Huntington's (Colomer *et al.* 1997) and Alzheimer's disease (Penzes & Remmers 2012). RNAi-dependent knockdown of kalirin in mice leads to reductions in the size of the cortex and cortical layers (Xie *et al.* 2010). Overexpression of kalirin-9 in the auditory cortex was found in schizophrenia patients compared with control subjects (Deo *et al.* 2012). The current finding provides further evidence for a role of *KALRN* in the development of auditory cortex.

The locus that showed the most significant association with the cortical thickness of left HG was located 12.63 kilobases away from the protein-coding gene *COBLL1* (cordon-bleu WH2 repeat protein-like 1) at 2q24.3. The Gene Ontology annotation for this gene is actin binding (GO:0003779, Gene Ontology Consortium *et al.* 2013). The protein cordon-bleu is involved in neural tube development (Carroll *et al.* 2003).

A large number of SNPs located on chromosome Xq21.1 were associated with the cortical thickness of right HG. These SNPs were located roughly 1 Mb upstream of the gene *POU3F4* (POU class 3 homeobox 4). *POU3F4* encodes a POU-domain neural transcription factor that is broadly expressed in the developing nervous system (He *et al.* 1989). Human *POU3F4* was the first causative gene identified for X-linked non-syndromic deafness (De Kok *et al.* 1995).

Table 2: SNPs associated with the cortical surface area of HG (pointwise $P < 1 \times 10^{-5}$)

Locus	No. SNPs	RSID	A1	Freq1	*P*	Direction	HetISq	Variance explained (%) BIG	SHIP-2	SHIP-T	Gene name	Gene distance
Surface area of left HG												
2p23.3	1	rs11892454	A	0.75	9.33E−06	−−−	4.5	0.99	0.15	0.43	*DTNB*	14 788
3q21.2	3	rs333332	T	0.33	**2.27E−06**	−−−	60	1.29	0.45	0.06	*KALRN*	0
4p15.1	3	rs67437545	A	0.82	4.44E−06	−−−	13.3	0.93	0.57	0.11	*ARAP2*	898 739
5q23.1	2	rs1032859	A	0.86	6.32E−06	−−−	0	0.80	0.34	0.34	*TNFAIP8*	0
10q22.1	1	rs4747241	T	0.38	7.37E−06	+++	14.1	1.02	0.14	0.46	*DDIT4*	632
15q15.1	2	rs78153629	T	0.88	4.99E−06	−−−	13.4	0.95	0.53	0.11	*KNSTRN*	1456
20q13.31	2	rs6064406	A	0.45	8.75E−06	+++	0	0.78	0.51	0.15	*RTFDC1*	0
	2	rs6069767	T	0.44	7.63E−06	+++	0	0.69	0.49	0.27	*GCNT7*	0
	1	rs28620942	A	0.55	7.61E−06	−−−	0	0.78	0.52	0.15	*FAM209A*	109
Surface area of right HG												
2p25.3	8	rs11885103	A	0.44	2.06E−06	−−−	61.2	1.17	0.48	0.05	*TMEM18*	73 606
3p25.1	2	rs13085837	A	0.12	1.47E−06	−−−	0	0.29	0.60	0.92	*SH3BP5*	21 302
3q12.1	21	rs72932726	A	0.11	**2.77E−07**	+++	0	0.86	0.46	0.50	*DCBLD2*	212 542
6q22.1	1	rs60678552	C	0.87	5.16E−06	+++	5	0.34	1.01	0.25	*DSE*	0
7q21.13	4	rs17301259	A	0.76	4.27E−06	+++	0	0.44	0.37	0.71	*ZNF804B*	0
	1	rs73215715	A	0.27	9.20E−06	+++	2	0.26	0.34	0.97	*DPY19L2P4*	120 078
9p22.2	1	rs1337391	A	0.08	8.78E−06	−−−	42.4	0.80	0.07	0.75	*BNC2*	0
10q26.2	1	rs10741159	T	0.21	9.94E−06	+++	0	0.81	0.23	0.32	*MKI67*	536 042
13q22.1	5	rs9573194	T	0.82	3.32E−06	−−−	78.6	0.05	1.63	0.48	*KLF12*	255 772
14q24.2	11	rs56193103	T	0.35	2.26E−06	+++	0	0.35	0.74	0.62	*PCNX*	91 053
14q31.2	1	rs10484157	T	0.11	4.83E−06	+++	0	0.51	0.44	0.53	*LOC101928599*	400 000
17q24.2	3	rs4791051	A	0.52	2.23E−06	−−−	67.5	0.20	0.30	1.65	*PRKCA*	0
18p11.32	4	rs56728521	A	0.92	6.99E−06	−−−	78.8	0.29	0.05	1.85	*METTL4*	553 102
18q21.1	5	rs75116816	C	0.79	1.97E−06	−−−	0	0.52	0.68	0.33	*ACAA2*	20 824
22q11.1	1	rs12484781	A	0.07	7.03E−06	+++	0	0.51	0.42	0.46	*IL17RA*	0
	1	rs971768	A	0.07	2.41E−06	+++	0	0.59	0.48	0.45	*CECR6*	0

Mouse models have indicated its essential role in inner ear development (Phippard *et al.* 1999, 2000). The expression of *POU3F4* during inner ear development depends on multiple regulatory elements (Naranjo *et al.* 2010). One of these is located 970 kb away from the gene, which overlaps with the locus associated to right HG thickness in our analysis. Further research is required to investigate the potential link between *POU3F4* and the development of primary auditory cortex.

We found no clear evidence for association between the HG measures and any of the candidate variants or genes that we queried, in relation to our hypotheses regarding pitch perception, cortical surface area, average cortical thickness, hearing loss and schizophrenia. One schizophrenia SNP (rs7085104) was marginally significantly associated with left HG area. However, individuals with more schizophrenia risk alleles for this SNP showed a larger HG area, which is in the opposite direction to the prediction based on previous findings.

Due to the large sample size in this study, it is necessary for us to use automatic segmentation and parcellation methods in imaging analysis (Desikan *et al.* 2006). These methods are not perfect in capturing all aspects of brain structures, especially when the gyrification pattern of a brain region is highly variable and complicated (Engel *et al.* 2011). This is especially relevant for the HG, as it can present as a single gyrus, a partially duplicated gyrus or a completely duplicated gyrus (Abdul-Kareem & Sluming 2008). Estimates of the probability of partial or complete duplications range from 30% (Abdul-Kareem & Sluming 2008) to 40% (Marie *et al.* 2012). We aimed to include the duplicated part as defined within the atlas; however, it was not successful in all cases. In an exploratory analysis, we selected eight subjects with a clear pattern of duplication in left HG from 262 randomly chosen subjects. The parcellation based on the Desikan atlas captured at least a substantial part of the second gyrus in six of them. This could be improved by developing more sophisticated parcellation protocols and introducing minimal manual interventions, provided that they are practically feasible for large datasets. An example of such a semi-automated method was developed by Schneider and colleagues (Schneider *et al.* 2005; Wengenroth *et al.* 2010, 2013). Future studies should investigate whether this method can scale up to larger sample size studies such as GWAS.

If the presence of a duplicated gyrus is well captured, an index of HG gyrification would be another interesting endophenotype for future analyses. Eckert and Leonard (1999) manually labeled the structure of HG in siblings and

Table 3: SNPs associated with the cortical thickness of HG (pointwise $P < 1 \times 10^{-5}$)

Locus	No. SNPs	RSID	A1	Freq1	*P*	Direction	HetISq	Variance explained (%) BIG	SHIP-2	SHIP-T	Gene name	Gene distance
Cortical thickness of left HG												
2q24.3	13	rs143000161	A	0.92	**2.40E−06**	−−−	0	0.73	0.49	0.67	*COBLL1*	12 612
	2	rs13021699	A	0.08	7.17E−06	+++	0	0.58	0.47	0.64	*SLC38A11*	26 000
3q27.2	2	rs9815925	A	0.89	8.71E−06	+++	0	0.39	0.67	0.68	*VPS8*	0
5q23.3	4	rs331079	C	0.09	5.17E−06	+++	36.4	1.17	0.50	0.13	*FBN2*	0
6p24.2	2	rs34698933	A	0.65	3.23E−06	+++	0	0.76	0.77	0.31	*SMIM13*	7922
7p21.3	3	rs6947964	T	0.44	6.18E−06	+++	0	0.88	0.60	0.23	*NDUFA4*	204 091
8p23.1	1	rs1293320	T	0.34	9.92E−06	+++	0	0.35	0.77	0.69	*FDFT1*	0
10q24.1	1	rs533480	A	0.29	9.67E−06	+++	34.5	0.54	1.31	0.13	*SORBS1*	0
11q14.3	1	rs13377206	A	0.83	2.72E−06	−−−	0	0.82	0.23	0.91	*MIR4490*	287 076
13q31.1	10	rs34073438	A	0.21	5.02E−06	+++	0	0.84	0.55	0.34	*SLITRK1*	319 946
16q21	1	rs77016911	C	0.06	9.58E−06	+++	45.6	0.53	0.11	1.42	*LOC283867*	69 114
Cortical thickness of right HG												
2q33.2	4	rs4675361	T	0.75	4.56E−06	−−−	0	0.61	0.53	0.70	*CD28*	0
3q25.1	1	rs1554120	A	0.85	5.25E−06	−−−	0	0.33	1.09	0.51	*MED12L*	0
4p15.2	7	rs6448317	T	0.19	3.99E−06	−−−	73	1.69	0.14	0.20	*CCDC149*	0
8p23.3	2	rs4876199	T	0.87	3.55E−06	−−−	71.2	0.92	0.02	1.43	*MYOM2*	83 530
Xq21.1	134	rs7062395	A	0.81	**2.38E−06**	+++	0	0.50	1.08	1.13	*POU3F4*	1 000 574

Tables 2 and 3 are sorted by genomic positions. Only the most significant SNP within each linkage disequilibrium block is reported. 'A1' refers to the reference allele. 'Direction' shows the direction of the β values from linear regression, in the order of BIG, SHIP-2 and SHIP-T. '+' indicates that the trait increases with the number of A1. 'HetISq' refers to the I^2 in the heterogeneity test. 'Variance explained' is calculated as $2pq \times \beta^2/(\mathrm{SD})^2$; p = MAF, $q = 1 - p$, β = unstandardized regression coefficient, SD = standard deviation of the phenotype without covariate corrections. 'Gene distance' is in the unit of base pairs (BP). Boldface indicates the lowest *P* value in the current GWAS. A full list of SNPs with $P < 1 \times 10^{-5}$ are provided in Table S1 with more details.

Table 4: Effect of rs72932726 on the surface areas of Desikan regions

Region names	NMISS	*P*	Direction	HetISq	HetPVal
rh_superior_frontal	3083	9.07E−08	+++	0	0.7701
rh_superior_temporal	3086	1.59E−07	+++	0	0.7089
rh_transverse_temporal	3085	4.67E−07	+++	0	0.9335
lh_superior_frontal	3086	1.45E−05	+++	0	0.5845
lh_middle_temporal	3088	1.71E−05	+++	0	0.4030
rh_pars_orbitalis	3087	6.00E−05	+++	0	0.6516
lh_insula	3068	2.38E−04	+++	31.5	0.2322
lh_rostral_anterior_cingulate	3090	3.26E−04	+++	42.5	0.1757
lh_transverse_temporal	3084	3.61E−04	+++	0	0.5038
lh_precuneus	3090	5.57E−04	+++	38.9	0.1944
lh_superior_temporal	3087	5.86E−04	+++	0	0.9623

'lh' and 'rh' in 'Region names' refer to left and right hemisphere, respectively. 'transverse_temporal' refers to HG in the Desikan atlas. 'NMISS' indicates the number of non-missing samples. 'Direction' shows the direction of the β values from linear regression, in the order of BIG, SHIP-2 and SHIP-T. '+' indicates that the surface area increases with the number of A1. 'HetIsq' and 'HetPVal' refer to the I^2 and *P* values in the heterogeneity test. The *P* values shown are not corrected for multiple comparisons, but they are significant after Bonferroni correction for all regions within the Desikan atlas. See Table S5 for the results for all regions, whether significant or not after Bonferroni correction.

found that the duplication pattern in the right HG was consistent with a traditional Mendelian dominant pattern of inheritance. Moreover, the gyrification pattern at birth predicts later functional development (Dubois *et al.* 2008). Finally, the fact that the shape of HG does not change substantially during adulthood (Golestani *et al.* 2011) suggests that gyrification could be a very interesting endophenotype, albeit difficult to compute automatically at present.

The population differences between the datasets used in this study might have prevented us from detecting the true genetic influences on HG. First, the age distributions differ between the datasets. The BIG project includes predominantly young adults while the age of participants in the SHIP project is much more evenly distributed across a broader age range. Previously, it has been shown that GM area of HG is significantly smaller in old adults (Torii *et al.* 2012). As a

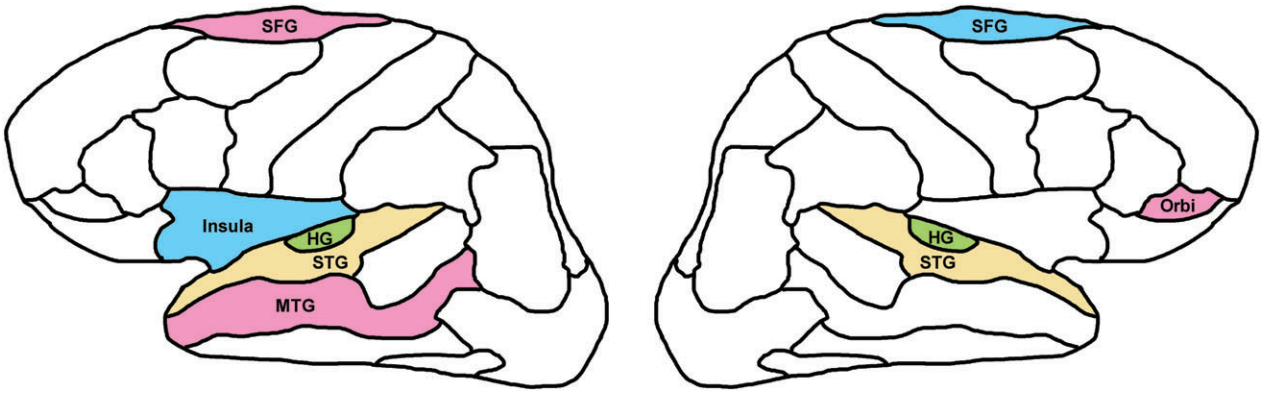

Figure 2: Brain regions showing significant association with rs72932726. The black lines indicate the boundaries between different brain regions from the Desikan atlas on the inflated surface (Desikan *et al*. 2006). Orbi, pars orbitalis. Bilateral HG (in green) and STG (in yellow) form the core part of the auditory network. Bilateral STG as well as left SFG, left MTG and right pars orbitalis (in pink) are involved in different stages of language processing. Left insula, right SFG (in blue) and another two regions (left rostral anterior cingulate and left precuneus, not shown in the figure) were also significantly associated with the SNP.

consequence, the age-related variation in HG surface area could have obscured genetic effects, for instance by an interaction of age with genetic factors. Second, there are differences in the education levels between participants from BIG (mostly university students) and from SHIP (general population). Although it is difficult to test, this could have led to a larger exposure to second language learning in the BIG sample, which might in turn affect the size of HG (Ressel *et al.* 2012).

In conclusion, we found a suggestive genetic variant (rs72932726) related to the surface area of right HG. Other regions connected to HG in the auditory and language networks also showed a significant association to the same variant. The variance in left HG area and thickness might be partly explained by the expression levels of *KALRN* and *COBLL1* in the auditory cortex, both of which regulate neuron morphogenesis. The right HG thickness is possibly related to the inner ear development which is regulated by the X-linked deafness gene *POU3F4*. Further studies are needed to confirm these hypotheses. Future work may require improved automated approaches in segmenting HG. Replication of the current findings in a larger sample will also be important.

References

Abdul-Kareem, I.A. & Sluming, V. (2008) Heschl gyrus and its included primary auditory cortex: structural MRI studies in healthy and diseased subjects. *J Magn Reson Imaging* **28**, 287–299.

Bakken, T.E., Bloss, C.S., Roddey, J.C., Joyner, A.H., Rimol, L.M., Djurovic, S., Melle, I., Sundet, K., Agartz, I., Andreassen, O.A., Dale, A.M. & Schork, N.J. (2011) Association of genetic variants on 15q12 with cortical thickness and cognition in schizophrenia. *Arch Gen Psychiatry* **68**, 781–790.

Barsh, G.S., Copenhaver, G.P., Gibson, G. & Williams, S.M. (2012) Guidelines for genome-wide association studies. *PLoS Genet* **8**, e1002812.

Carroll, E.A., Gerrelli, D., Gasca, S., Berg, E., Beier, D.R., Copp, A.J. & Klingensmith, J. (2003) Cordon-bleu is a conserved gene involved in neural tube formation. *Dev Biol* **262**, 16–31.

Chen, Y., Low, T.Y., Choong, L.Y., Ray, R.S., Tan, Y.L., Toy, W., Lin, Q., Ang, B.K., Wong, C.H., Lim, S., Li, B., Hew, C.L., Sze, N.S., Druker, B.J. & Lim, Y.P. (2007) Phosphoproteomics identified Endofin, DCBLD2, and KIAA0582 as novel tyrosine phosphorylation targets of EGF signaling and Iressa in human cancer cells. *Proteomics* **7**, 2384–2397.

Colomer, V., Engelender, S., Sharp, A.H., Duan, K., Cooper, J.K., Lanahan, A., Lyford, G., Worley, P. & Ross, C.A. (1997) Huntingtin-associated protein 1 (HAP1) binds to a Trio-like polypeptide, with a rac1 guanine nucleotide exchange factor domain. *Hum Mol Genet* **6**, 1519–1525.

Da Costa, S., van der Zwaag, W., Marques, J.P., Frackowiak, R.S., Clarke, S. & Saenz, M. (2011) Human primary auditory cortex follows the shape of Heschl's gyrus. *J Neurosci* **31**, 14067–14075.

Dediu, D. & Ladd, D.R. (2007) Linguistic tone is related to the population frequency of the adaptive haplogroups of two brain size genes, ASPM and Microcephalin. *Proc Natl Acad Sci USA* **104**, 10944–10949.

Deo, A.J., Cahill, M.E., Li, S., Goldszer, I., Henteleff, R., Vanleeuwen, J.E., Rafalovich, I., Gao, R., Stachowski, E.K., Sampson, A.R., Lewis, D.A., Penzes, P. & Sweet, R.A. (2012) Increased expression of Kalirin-9 in the auditory cortex of schizophrenia subjects: its role in dendritic pathology. *Neurobiol Dis* **45**, 796–803.

Desikan, R.S., Segonne, F., Fischl, B., Quinn, B.T., Dickerson, B.C., Blacker, D., Buckner, R.L., Dale, A.M., Maguire, R.P., Hyman, B.T., Albert, M.S. & Killiany, R.J. (2006) An automated labeling system for subdividing the human cerebral cortex on MRI scans into gyral based regions of interest. *Neuroimage* **31**, 968–980.

Dubois, J., Benders, M., Borradori-Tolsa, C., Cachia, A., Lazeyras, F., Ha-Vinh Leuchter, R., Sizonenko, S.V., Warfield, S.K., Mangin, J.F. & Huppi, P.S. (2008) Primary cortical folding in the human newborn: an early marker of later functional development. *Brain* **131**, 2028–2041.

Eckert, M.A. & Leonard, C.M. (1999) Heritability of Heschl's gyrus duplication: a neural risk factor for dyslexia. *J Cogn Neurosci* **10**, 99–99.

Emmorey, K., Allen, J.S., Bruss, J., Schenker, N. & Damasio, H. (2003) A morphometric analysis of auditory brain regions in congenitally deaf adults. *Proc Natl Acad Sci USA* **100**, 10049–10054.

Engel, K., Toennies, K.D. & Brechmann, A. (2011) Part-based localisation and segmentation of landmark-related auditory cortical regions. *Pattern Recognit* **44**, 2017–2033.

Eyler, L.T., Chen, C.H., Panizzon, M.S., Fennema-Notestine, C., Neale, M.C., Jak, A., Jernigan, T.L., Fischl, B., Franz, C.E., Lyons, M.J.,

Grant, M., Prom-Wormley, E., Seidman, L.J., Tsuang, M.T., Fiecas, M.J., Dale, A.M. & Kremen, W.S. (2012) A comparison of heritability maps of cortical surface area and thickness and the influence of adjustment for whole brain measures: a magnetic resonance imaging twin study. *Twin Res Hum Genet* **15**, 304–314.

Ferreira, M.A. & Purcell, S.M. (2009) A multivariate test of association. *Bioinformatics* **25**, 132–133.

Fischl, B., van der Kouwe, A., Destrieux, C., Halgren, E., Segonne, F., Salat, D.H., Busa, E., Seidman, L.J., Goldstein, J., Kennedy, D., Caviness, V., Makris, N., Rosen, B. & Dale, A.M. (2004) Automatically parcellating the human cerebral cortex. *Cereb Cortex* **14**, 11–22.

Franke, B., Vasquez, A.A., Veltman, J.A., Brunner, H.G., Rijpkema, M. & Fernández, G. (2010) Genetic variation in CACNA1C, a gene associated with bipolar disorder, influences brainstem rather than gray matter volume in healthy individuals. *Biol Psychiatry* **68**, 586–588.

Gandour, J., Wong, D. & Hutchins, G. (1998) Pitch processing in the human brain is influenced by language experience. *Neuroreport* **9**, 2115–2119.

Gaser, C. & Schlaug, G. (2003) Brain structures differ between musicians and non-musicians. *J Neurosci* **23**, 9240–9245.

Gaser, C., Nenadic, I., Volz, H.P., Buchel, C. & Sauer, H. (2004) Neuroanatomy of "hearing voices": a frontotemporal brain structural abnormality associated with auditory hallucinations in schizophrenia. *Cereb Cortex* **14**, 91–96.

Gene Ontology Consortium, Blake, J.A., Dolan, M. *et al.* (2013) Gene Ontology annotations and resources. *Nucleic Acids Res* **41**, D530–D535.

Glausier, J.R. & Lewis, D.A. (2013) Dendritic spine pathology in schizophrenia. *Neuroscience* **251**, 90–107.

Golestani, N. & Pallier, C. (2007) Anatomical correlates of foreign speech sound production. *Cereb Cortex* **17**, 929–934.

Golestani, N., Price, C.J. & Scott, S.K. (2011) Born with an ear for dialects? Structural plasticity in the expert phonetician brain. *J Neurosci* **31**, 4213–4220.

Guadalupe, T., Zwiers, M.P., Teumer, A., Wittfeld, K., Vasquez, A.A., Hoogman, M., Hagoort, P., Fernandez, G., Buitelaar, J., Hegenscheid, K., Völzke, H., Franke, B., Fisher, S.E., Grabe, H.J. & Francks, C. (2014) Measurement and genetics of human subcortical and hippocampal asymmetries in large datasets. *Hum Brain Mapp* **35**, 3277–3289.

Hart, H.C., Palmer, A.R. & Hall, D.A. (2002) Heschl's gyrus is more sensitive to tone level than non-primary auditory cortex. *Hear Res* **171**, 177–190.

He, X., Treacy, M.N., Simmons, D.M., Ingraham, H.A., Swanson, L.W. & Rosenfeld, M.G. (1989) Expression of a large family of POU-domain regulatory genes in mammalian brain development. *Nature* **340**, 35–41.

Hegenscheid, K., Kuhn, J.P., Volzke, H., Biffar, R., Hosten, N. & Puls, R. (2009) Whole-body magnetic resonance imaging of healthy volunteers: pilot study results from the population-based SHIP study. *RoFo* **181**, 748–759.

Hickok, G. & Poeppel, D. (2007) The cortical organization of speech processing. *Nat Rev Neurosci* **8**, 393–402.

Hilgert, N., Smith, R.J.H. & Van Camp, G. (2009) Forty-six genes causing nonsyndromic hearing impairment: which ones should be analyzed in DNA diagnostics? *Mutat Res* **681**, 189–196.

Joyner, A.H., Roddey, J.C., Bloss, C.S., Bakken, T.E., Rimol, L.M., Melle, I., Agartz, I., Djurovic, S., Topol, E.J., Schork, N.J., Andreassen, O.A. & Dale, A.M. (2009) A common MECP2 haplotype associates with reduced cortical surface area in humans in two independent populations. *Proc Natl Acad Sci USA* **106**, 15483–15488.

Kang, J., Wang, L., Yan, C.G., Wang, J.H., Liang, X. & He, Y. (2011) Characterizing dynamic functional connectivity in the resting brain using variable parameter regression and Kalman filtering approaches. *Neuroimage* **56**, 1222–1234.

Kobuke, K., Furukawa, Y., Sugai, M., Tanigaki, K., Ohashi, N., Matsumori, A., Sasayama, S., Honjo, T. & Tashiro, K. (2001) ESDN, a novel neuropilin-like membrane protein cloned from vascular cells with the longest secretory signal sequence among eukaryotes, is up-regulated after vascular injury. *J Biol Chem* **276**, 34105–34114.

Kochunov, P., Glahn, D.C., Nichols, T.E., Winkler, A.M., Hong, E.L., Holcomb, H.H., Stein, J.L., Thompson, P.M., Curran, J.E., Carless, M.A., Olvera, R.L., Johnson, M.P., Cole, S.A., Kochunov, V., Kent, J. & Blangero, J. (2011) Genetic analysis of cortical thickness and fractional anisotropy of water diffusion in the brain. *Front Neurosci* **5**, 120.

de Kok, Y.J., van der Maarel, S.M., Bitner-Glindzicz, M., Huber, I., Monaco, A.P., Malcolm, S., Pembrey, M.E., Ropers, H.H. & Cremers, F.P. (1995) Association between X-linked mixed deafness and mutations in the POU domain gene POU3F4. *Science* **267**, 685–688.

Krumbholz, K., Patterson, R.D., Seither-Preisler, A., Lammertmann, C. & Lutkenhoner, B. (2003) Neuromagnetic evidence for a pitch processing center in Heschl's gyrus. *Cereb Cortex* **13**, 765–772.

Lamminmaki, S., Massinen, S., Nopola-Hemmi, J., Kere, J. & Hari, R. (2012) Human ROBO1 regulates interaural interaction in auditory pathways. *J Neurosci* **32**, 966–971.

Li, J., Cheng, J., Lu, Y., Lu, Y., Chen, A., Sun, Y., Kang, D., Zhang, X., Dai, P., Han, D. & Yuan, H. (2010) Identification of a novel mutation in POU3F4 for prenatal diagnosis in a Chinese family with X-linked nonsyndromic hearing loss. *J Genet Genomics* **37**, 787–793.

Li, M.-X., Gui, H.-S., Kwan, Johnny S.H. & Sham, Pak C. (2011) GATES: a rapid and powerful gene-based association test using extended Simes procedure. *Am J Hum Genet* **88**, 283–293.

Marie, D., Hervé, P.-Y., Petit, L., Crivello, F., Jobard, G., Zago, L., Mellet, E., Mazoyer, B. & Tzourio-Mazoyer, N. (2012) Morphology and surface area of Heschl's gyri in 232 right and 198 left-handers. Poster presented at the 18th *Organization for Human Brain Mapping*. Beijing.

May, V., Schiller, M.R., Eipper, B.A. & Mains, R.E. (2002) Kalirin Dbl-homology guanine nucleotide exchange factor 1 domain initiates new axon outgrowths via RhoG-mediated mechanisms. *J Neurosci* **22**, 6980–6990.

Menenti, L., Petersson, K.M., Scheeringa, R. & Hagoort, P. (2009) When elephants fly: differential sensitivity of right and left inferior frontal gyri to discourse and world knowledge. *J Cogn Neurosci* **21**, 2358–2368.

Morosan, P., Rademacher, J., Schleicher, A., Amunts, K., Schormann, T. & Zilles, K. (2001) Human primary auditory cortex: cytoarchitectonic subdivisions and mapping into a spatial reference system. *Neuroimage* **13**, 684–701.

Naranjo, S., Voesenek, K., de la Calle-Mustienes, E., Robert-Moreno, A., Kokotas, H., Grigoriadou, M., Economides, J., Van Camp, G., Hilgert, N., Moreno, F., Alsina, B., Petersen, M.B., Kremer, H. & Gomez-Skarmeta, J.L. (2010) Multiple enhancers located in a 1-Mb region upstream of POU3F4 promote expression during inner ear development and may be required for hearing. *Hum Genet* **128**, 411–419.

Oikkonen, J., Huang, Y., Onkamo, P., Ukkola-Vuoti, L., Raijas, P., Karma, K., Vieland, V.J. & Jarvela, I. (2014) A genome-wide linkage and association study of musical aptitude identifies loci containing genes related to inner ear development and neurocognitive functions. *Mol Psychiatry*. DOI:10.1038/mp.2014.8.

Panizzon, M.S., Fennema-Notestine, C., Eyler, L.T., Jernigan, T.L., Prom-Wormley, E., Neale, M., Jacobson, K., Lyons, M.J., Grant, M.D., Franz, C.E., Xian, H., Tsuang, M., Fischl, B., Seidman, L., Dale, A. & Kremen, W.S. (2009) Distinct genetic influences on cortical surface area and cortical thickness. *Cereb Cortex* **19**, 2728–2735.

Patterson, R.D., Uppenkamp, S., Johnsrude, I.S. & Griffiths, T.D. (2002) The processing of temporal pitch and melody information in auditory cortex. *Neuron* **36**, 767–776.

Peng, G., Deutsch, D., Henthorn, T., Su, D. & Wang, W.S.-Y. (2013) Language experience influences non-linguistic pitch perception. *J Chin Linguist* **41**, 447–467.

Penhune, V.B., Zatorre, R.J., MacDonald, J.D. & Evans, A.C. (1996) Interhemispheric anatomical differences in human primary auditory

cortex: probabilistic mapping and volume measurement from magnetic resonance scans. *Cereb Cortex* **6**, 661–672.
Penzes, P. & Remmers, C. (2012) Kalirin signaling: implications for synaptic pathology. *Mol Neurobiol* **45**, 109–118.
Peper, J.S., Brouwer, R.M., Boomsma, D.I., Kahn, R.S. & Hulshoff Pol, H.E. (2007) Genetic influences on human brain structure: a review of brain imaging studies in twins. *Hum Brain Mapp* **28**, 464–473.
Phippard, D., Lu, L., Lee, D., Saunders, J.C. & Crenshaw, E.B. 3rd (1999) Targeted mutagenesis of the POU-domain gene Brn4/Pou3f4 causes developmental defects in the inner ear. *J Neurosci* **19**, 5980–5989.
Phippard, D., Boyd, Y., Reed, V., Fisher, G., Masson, W.K., Evans, E.P., Saunders, J.C. & Crenshaw, E.B. 3rd (2000) The sex-linked fidget mutation abolishes Brn4/Pou3f4 gene expression in the embryonic inner ear. *Hum Mol Genet* **9**, 79–85.
Price, C.J. (2012) A review and synthesis of the first 20 years of PET and fMRI studies of heard speech, spoken language and reading. *Neuroimage* **62**, 816–847.
Purcell, S., Cherny, S.S. & Sham, P.C. (2003) Genetic Power Calculator: design of linkage and association genetic mapping studies of complex traits. *Bioinformatics* **19**, 149–150.
Purcell, S., Neale, B., Todd-Brown, K., Thomas, L., Ferreira, M.A.R., Bender, D., Maller, J., Sklar, P., de Bakker, P.I.W., Daly, M.J. & Sham, P.C. (2007) PLINK: a tool set for whole-genome association and population-based linkage analyses. *Am J Hum Genet* **81**, 559–575.
Purcell, S., Wray, N.R., Stone, J.L., Visscher, P.M., O'Donovan, M.C., Sullivan, P.F. & Sklar, P. (2009) Common polygenic variation contributes to risk of schizophrenia and bipolar disorder. *Nature* **460**, 748–752.
Puschmann, S., Uppenkamp, S., Kollmeier, B. & Thiel, C.M. (2010) Dichotic pitch activates pitch processing centre in Heschl's gyrus. *Neuroimage* **49**, 1641–1649.
Rabiner, C.A., Mains, R.E. & Eipper, B.A. (2005) Kalirin: a dual Rho guanine nucleotide exchange factor that is so much more than the sum of its many parts. *Neuroscientist* **11**, 148–160.
Renvall, H., Salmela, E., Vihla, M., Illman, M., Leinonen, E., Kere, J. & Salmelin, R. (2012) Genome-wide linkage analysis of human auditory cortical activation suggests distinct loci on chromosomes 2, 3, and 8. *J Neurosci* **32**, 14511–14518.
Ressel, V., Pallier, C., Ventura-Campos, N., Diaz, B., Roessler, A., Avila, C. & Sebastian-Galles, N. (2012) An effect of bilingualism on the auditory cortex. *J Neurosci* **32**, 16597–16601.
Ripke, S., O'Dushlaine, C., Chambert, K. *et al.* (2013) Genome-wide association analysis identifies 13 new risk loci for schizophrenia. *Nat Genet* **45**, 1150–1159.
Sadeghi, M.M., Esmailzadeh, L., Zhang, J., Guo, X., Asadi, A., Krassilnikova, S., Fassaei, H.R., Luo, G., Al-Lamki, R.S., Takahashi, T., Tellides, G., Bender, J.R. & Rodriguez, E.R. (2007) ESDN is a marker of vascular remodeling and regulator of cell proliferation in graft arteriosclerosis. *Am J Transplant* **7**, 2098–2105.
Schneider, P., Scherg, M., Dosch, H.G., Specht, H.J., Gutschalk, A. & Rupp, A. (2002) Morphology of Heschl's gyrus reflects enhanced activation in the auditory cortex of musicians. *Nat Neurosci* **5**, 688–694.
Schneider, P., Sluming, V., Roberts, N., Scherg, M., Goebel, R., Specht, H.J., Dosch, H.G., Bleeck, S., Stippich, C. & Rupp, A. (2005) Structural and functional asymmetry of lateral Heschl's gyrus reflects pitch perception preference. *Nat Neurosci* **8**, 1241–1247.
Scott, S.K., Leff, A.P. & Wise, R.J. (2003) Going beyond the information given: a neural system supporting semantic interpretation. *Neuroimage* **19**, 870–876.
Smiley, J.F. (2009) Auditory cortex anatomy and asymmetry in schizophrenia. In Lajtha, A., Javitt, D. & Kantrowitz, J. (eds), *Handbook of Neurochemistry and Molecular Neurobiology*. Springer, New York, NY, pp. 353–381.
Smiley, J.F., Hackett, T.A., Preuss, T.M., Bleiwas, C., Figarsky, K., Mann, J.J., Rosoklija, G., Javitt, D.C. & Dwork, A.J. (2013) Hemispheric asymmetry of primary auditory cortex and Heschl's gyrus in schizophrenia and nonpsychiatric brains. *Psychiatry Res* **214**, 435–443.
Stein, J.L., Medland, S.E., Vasquez, A.A. *et al.* (2012) Identification of common variants associated with human hippocampal and intracranial volumes. *Nat Genet* **44**, 552–561.
Teumer, A., Holtfreter, B., Volker, U., Petersmann, A., Nauck, M., Biffar, R., Volzke, H., Kroemer, H.K., Meisel, P., Homuth, G. & Kocher, T. (2013) Genome-wide association study of chronic periodontitis in a general German population. *J Clin Periodontol* **40**, 977–985.
Torii, Y., Iritani, S., Sekiguchi, H., Habuchi, C., Hagikura, M., Arai, T., Ikeda, K., Akiyama, H. & Ozaki, N. (2012) Effects of aging on the morphologies of Heschl's gyrus and the superior temporal gyrus in schizophrenia: a postmortem study. *Schizophr Res* **134**, 137–142.
Volzke, H., Alte, D., Schmidt, C.O. *et al.* (2011) Cohort profile: the study of health in Pomerania. *Int J Epidemiol* **40**, 294–307.
Wengenroth, M., Blatow, M., Bendszus, M. & Schneider, P. (2010) Leftward lateralization of auditory cortex underlies holistic sound perception in Williams syndrome. *PLoS One* **5**, e12326.
Wengenroth, M., Blatow, M., Heinecke, A., Reinhardt, J., Stippich, C., Hofmann, E. & Schneider, P. (2013) Increased volume and function of right auditory cortex as a marker for absolute pitch. *Cereb Cortex* **24**, 1127–1137.
Willer, C.J., Li, Y. & Abecasis, G.R. (2010) METAL: fast and efficient meta-analysis of genomewide association scans. *Bioinformatics* **26**, 2190–2191.
Winkler, A.M., Kochunov, P., Blangero, J., Almasy, L., Zilles, K., Fox, P.T., Duggirala, R. & Glahn, D.C. (2010) Cortical thickness or grey matter volume? The importance of selecting the phenotype for imaging genetics studies. *Neuroimage* **53**, 1135–1146.
Wong, P.C., Warrier, C.M., Penhune, V.B., Roy, A.K., Sadehh, A., Parrish, T.B. & Zatorre, R.J. (2008) Volume of left Heschl's Gyrus and linguistic pitch learning. *Cereb Cortex* **18**, 828–836.
Wong, P.C., Chandrasekaran, B. & Zheng, J. (2012) The derived allele of ASPM is associated with lexical tone perception. *PLoS One* **7**, e34243.
Xie, Z., Cahill, M.E. & Penzes, P. (2010) Kalirin loss results in cortical morphological alterations. *Mol Cell Neurosci* **43**, 81–89.

Acknowledgements

BIG: We wish to thank all persons who kindly participated in the BIG (Brain Imaging Genetics) research. This work makes use of the BIG dataset, first established in Nijmegen, The Netherlands, in 2007. This resource is now part of Cognomics (www.cognomics.nl), a joint initiative by researchers of the Donders Centre for Cognitive Neuroimaging, the Human Genetics and Cognitive Neuroscience departments of the Radboud University Nijmegen Medical Centre and the Max Planck Institute for Psycholinguistics in Nijmegen. The Cognomics Initiative is supported by the participating departments and centers and by external grants, i.e. the Biobanking and Biomolecular Resources Research Infrastructure (the Netherlands) (BBMRI-NL), the Hersenstichting Nederland, and the Netherlands Organisation for Scientific Research (NWO).

SHIP: The Study of Health in Pomerania (SHIP) is supported by the German Federal Ministry of Education and Research (grants 01ZZ9603, 01ZZ0103 and 01ZZ0403). Genome-wide data and MRI scans were supported by a joint grant from Siemens Healthcare, Erlangen, Germany, and the Federal State of Mecklenburg-West Pomerania. The University of Greifswald is a member of the Caché Campus program of the InterSystems GmbH.

SHIP-TREND: The authors from SHIP are grateful to M. Stanke for the opportunity to use his Server Cluster for SNP Imputation as well as to Holger Prokisch and Thomas Meitinger (Helmholtz Zentrum München) for the genotyping of the SHIP-TREND cohort that was supported by the Federal Ministry of Education and

Research (grant 03ZIK012). This cohort is part of the Community Medicine Research (CMR) net of the University of Greifswald, which is funded by the German Federal Ministry of Education and Research and the German Ministry of Cultural Affairs, as well as by the Social Ministry of the Federal State of Mecklenburg-West Pomerania (grant nos 01ZZ9603, 01ZZ0103 and 01ZZ0403). Magnetic resonance imaging scans were supported by the Federal Ministry of Education and Research and a joint grant from Siemens Healthcare, Erlangen, Germany, and the Federal State of Mecklenburg-West Pomerania.

No conflicts of interest are declared.

Supporting Information

Additional supporting information may be found in the online version of this article at the publisher's web-site:

Figure S1: Manhattan plots for individual datasets.

Figure S2: QQ plots for individual datasets and meta-analysis.

Figure S3: Correlations between the schizophrenia genetic risk score and the HG measures in 1004 participants from the BIG dataset.

Table S1: SNPs associated with the cortical surface area and thickness of Heschl's gyrus.

Table S2: Results of candidate gene analysis on pitch and cortical traits.

Table S3: Results of candidate gene analysis on hearing loss.

Table S4: Results of candidate gene analysis on schizophrenia.

Table S5: Effect of rs72932726 on the surface areas of 68 Desikan regions.